Available online at www.sciencedirect.com

ScienceDirect

Physics Procedia 56 (2014) 147 – 156

Physics Procedia

8th International Conference on Photonic Technologies LANE 2014

Performance limitations in polymer laser sintering

David L. Bourell[a,]*, Trevor J. Watt[a], David K. Leigh[a,b], Ben Fulcher[b]

[a] *Department of Mechanical Engineering, The University of Texas at Austin, Austin, TX 78712, United States*
[b] *Harvest Technologies, Belton, TX 76513, United States*

Abstract

Commercial laser sintering (LS) machines have been used for years in a variety of rapid prototyping applications. Emphasis in the LS research community has moved towards rapid manufacturing: the creation of engineered structural components. However, the mechanical properties of LS parts are often inconsistent compared to their molded counterparts. This is due to a variety of factors including feedstock uniformity, microstructure evolution due to LS processing, and the overall ability of commercial LS machines to reliably form structural parts without thermal degradation of the feedstock powder. This paper will review the current state of the art of commercial LS machines, and discuss the resulting implications for rapid manufacturing. Particular focus will be paid to the role of part bed temperature variations due to non-uniform heating, unsteady cooling due to natural convection currents in the part chamber, and how these and other phenomena may impact the design of laser control systems.

Peer-review under responsibility of the Bayerisches Laserzentrum GmbH

Keywords: polymer laser sintering; mechanical properties; microstructure; temperature monitoring; system improvements

1. Introduction

Over the past 25 years, various additive manufacturing techniques have been developed and grown into viable options for prototyping and production applications. Among these techniques, laser sintering (LS) of polymers is one of the most promising due to its ability to produce geometrically complex, dimensionally accurate parts with good mechanical strength. An illustration of the laser sintering process is shown in Fig. 1. Feedstock powder is

* Corresponding author. Tel.: +1-512-471-3170; fax: +1-512-471-7681 .
E-mail address: dbourell@mail.utexas.edu

Peer-review under responsibility of the Bayerisches Laserzentrum GmbH
doi:10.1016/j.phpro.2014.08.157

loaded into heated delivery chambers or "feed bins". The part piston lowers a predetermined amount and a roller or recoating blade spreads powder from the feed bins over the part bed. The part bed temperature is heated to just below the melt temperature to minimize the required laser energy and resulting part distortion during cooling. A carbon dioxide (CO_2) laser then heats the exposed powder according to the prescribed geometry, and the process repeats itself until the part is complete. Once the part is made, the heaters are turned off and the part bed gradually cools. This entire process takes place in a nitrogen atmosphere to prevent oxidation of the powder. Once the material in the part chamber, or "part cake", is cooled below the glass transition and oxidation temperatures, it is removed from the chamber and the loose powder is removed from the completed parts.

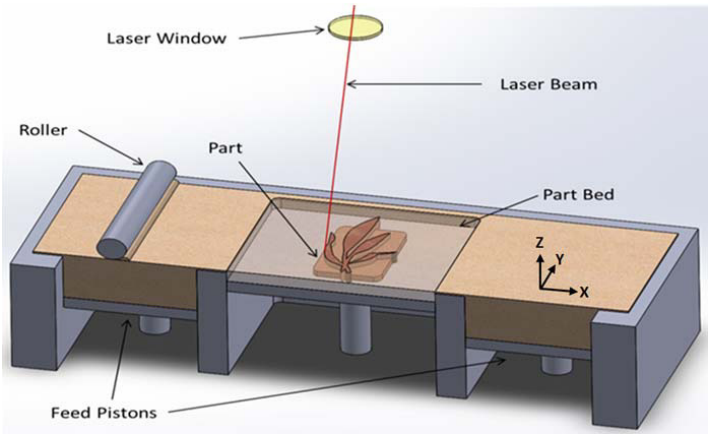

Fig. 1. SLS process illustration.

The laser sintering process is sensitive to a large number of physical parameters. First, a dry powder must have adequate flow characteristics to produce a smooth layer when displaced by a roller or other spreading mechanism. The powder must then absorb enough laser energy to reach a fully melted state necessary for complete bonding between powder particles, without the temperature of the surrounding powder becoming hot enough for thermal degradation to occur, as discussed in Starr et al. (2011) and Jain et al. (2009). The resulting viscosity of the molten polymer must also be low enough for it to completely fill inter-particle gaps, but high enough to prevent the molten material from sinking into the supporting powder bed, creating "sinkhole" porosity.

LS build parameters include part bed temperature, feed bed temperature, powder layer thickness, laser power, scan spacing, number of scans, time between layers, roller speed, build size, and heating/cooling rates; see Gibson and Shi (1997), and Liu-Lan et al. (2003). The density and mechanical behavior of LS parts are nominally a function of the accumulated laser energy density, part bed temperature (T_b), and part orientation, as discussed by Caulfield et al. (2007). The primary LS variable studied in the literature is laser power, or laser energy density. The correct laser energy setting depends on the part bed temperature, with a higher bed temperature requiring less laser energy to melt the powder. However, too high a part bed temperature can result in undesired bonding and a hard part cake, while too low a T_b can result in warping and insufficient melting, as discussed by Tontowi and Childs (2001). T_b is usually set 3-4°C below the melt temperature for semicrystalline polymers.

Both LS and injection molding (IM) produce parts with similar yield strengths, though the ductility of LS is generally an order of magnitude lower than IM parts as shown by Ajoku et al. (2006) and Griessbach et al. (2010). IM parts have a fundamentally different microstructure than LS parts, since IM parts experience shear stresses during processing that result in aligned lamellar crystalline regions and inter-twined molecular chains, see Zhou (2013). Rapid cooling in IM also results in reduced crystallinity compared to LS parts, as discussed by Hooreweder et al. (2013). Other phenomena that occur in LS are the formation of porosity, regular porosity between powder layers resulting in weak planar interfaces, and the presence of particle "cores" of a different crystallographic nature than the surrounding crystal structure; see Majewski et al. (2008).

For many years the presence of porosity and other microstructural defects limited LS primarily to prototype hardware, or for use as investment casting patterns. However, there has long been a desire to use additive manufacturing for the production of structural components. The use of polyamide 11 (PA 11) for laser sintered

prototypes at Rocketdyne (eventually acquired by Boeing) led the engineering staff to work with functional prototypes on experimental aircraft. Initial work on missile covers, laser turrets, and mounting hardware led the teams to investigate the possibility for laser sintering to be a solution for low volume and production applications as discussed by Hopkinson et al. (2006). Laser sintering was then introduced in the late 1990s as a manufacturing solution for end-use parts in the aerospace sector by Boeing and NavAir to supply low pressure ducting for the Boeing FA-18 aircraft. However, the resulting supply chain specifications created a significant barrier to entry for the laser sintering process. In recent years, and especially since the creation of America Makes: National Additive Manufacturing Innovation Institute (NAMII) in 2013, focus has again turned towards using additive manufacturing for the creation of structural parts.

Fig. 2 displays tensile data for 3500 production-grade laser sintered parts using Nylon 11 Arkema D80, tested at Harvest Technologies (Belton, TX, USA). X and Y are the powder layer in-plane directions, while Z is the out-of-plane direction (see coordinate system in Fig. 1). The Z-direction yield and tensile strength data show minor variability, around 10%. The strength of these LS parts is similar to IM parts. Elongation at fracture data for Z tensile bars show significant scatter, and the values are about an order of magnitude lower than typical values for IM parts. Most researchers attribute this behavior to particle coring, periodic porosity, and inter-layer porosity that can result in particularly poor properties in the Z direction. These problems primarily arise as a result of inconsistent powder deposition and incomplete particle melting. Incomplete melting is complicated by the fact that commercial LS machines often have uneven heating and cooling of the powder bed surface. This gives rise to local hot and cold spots that can result in insufficient heating (porosity, particle coring), or excessive heating (thermal degradation).

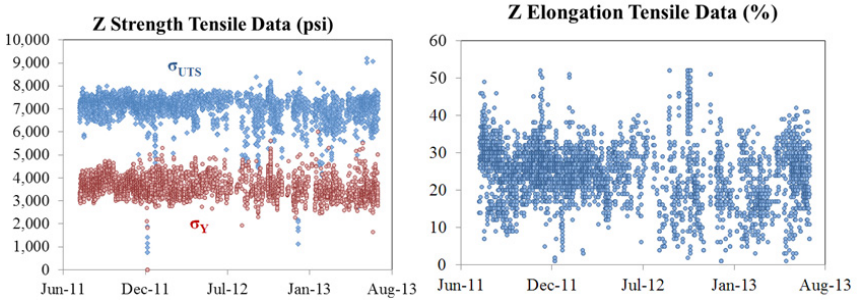

Fig. 2. PA11 strength and elongation data collected at Harvest Technologies, Inc.

Commercial polymer LS machines are only made by a few companies. These include 3D Systems (3DS, USA), ASPECT (Japan), EOS (Germany), and Hunan Farsoon (China). In recent years, digital scanning upgrades by EOS, 3DS, and Integra (USA) have significantly improved productivity. New multi-zone heaters have also been developed by Integra that allow for more consistent part bed temperatures. However, there has been little work to develop advanced laser control schemes that will likely be required for LS polymer parts to obtain a ductility approaching their injection-molded counterparts.

2. Properties of LS feedstock materials

LS polymer feedstock materials tend to be semi-crystalline polymers such as polyamide (PA, or “nylon”), and more recently polystyrene (PS), polyetheretherketone (PEEK), and polyether block amide (PEBA). Semi-crystalline polymers have large regions of crystalline order connected by short amorphous regions. Crystallites usually take the form of spherical crystals termed “spherulites” which grow out of distinct nuclei during solidification, with the number of nuclei increasing with increasing undercooling below the melting point as discussed by Argon (2013). Therefore, semi-crystalline polymers that are cooled quickly will have a greater number of smaller spherulites throughout the microstructure, as shown by Bessell et al. (1975).

Many semi-crystalline polymers form multiple crystal phases depending on the monomer unit length (e.g. PA6 vs. PA12) and the conditions of solidification. Polyamides can form α (monoclinic) and γ (hexagonal) phases, with α-PA forming under slow cooling rates or high temperatures, and γ-PA forming under fast cooling rates or low temperatures; see Huang et al. (2012). The overall extent of crystallinity affects both the density of the final

material, as well as the melting behavior. Melting behavior is usually measured with a differential scanning calorimeter (DSC), with example results shown in Fig. 3 for the heating (downward hump) and cooling (upward hump) cycles. The location and magnitude of DSC peaks may be used to identify the presence and relative quantity of different crystal phases, though this can be confounded by changing molecular weight distributions.

The location of the DSC peaks is also used to determine the operating window of the LS process. Typically, the part bed is kept 2-4 °C below the melt peak. This reduces the required laser energy to melt the powder, but it also prevents the molten polymer from crystallizing, causing localized solidification shrinkage and part distortion. The distance between the melt and recrystallization peaks is therefore the processing window for the part bed (see Fig. 3). If the part bed temperature is too high, melting of low molecular weight regions will result in a hard part cake and poor dimensional accuracy. If the part bed temperature is too low, insufficient melting can result in high part porosity, or crystallization can occur resulting in a warped part. One of the reasons that Nylon 11 and Nylon 12 are the dominant LS powders is their large processing windows.

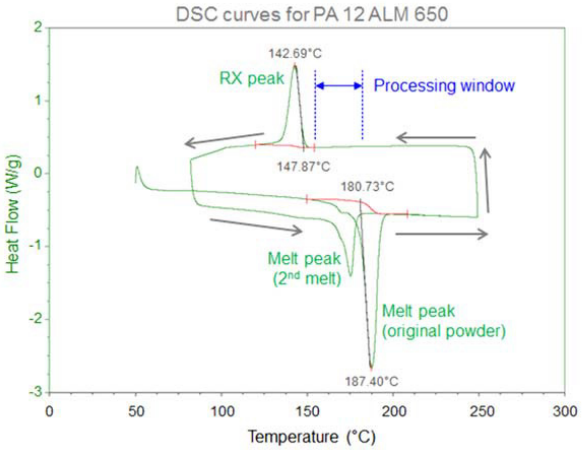

Fig. 3. Experimental DSC curve for PA12 powder collected at Harvest Technologies, Inc.

The separation between melt and crystallization temperatures gives rise to a curious aspect of LS: A "sintered" location will remain liquid until the entire part bed begins to cool later in the production cycle, as discussed by Kruth et al. (2007). The part bed will either be kept at an elevated temperature using piston heaters underneath the part bed, or will be cooled gradually once a location is far enough away from the part bed surface. Cooling rates are limited by conduction through the powder bed, which takes place very slowly due to the poor thermal conductivity of the polymer powder combined with thermal contact resistance between powder particles, as discussed by Yuan et al. (2011). This slow cooling, which can take many hours, gives rise to some of the disparate properties of LS parts compared to IM parts which solidify in a matter of seconds.

The optimum particle size for LS processing ability is 45-90 μm, as discussed by Goodridge et al. (2012). This is based on having as small a powder as possible to produce fine features, without agglomeration or triboelectric charging problems as discussed by Beaman et al. (1997). Particle shape affects powder flowability, powder bed density, part surface roughness, and final part porosity. Irregular particles tend to result in larger irregular voids compared to granular particles as shown by Yusoff et al. (2011), and LS parts tend to have poor elongation-to-fracture due in part to this residual porosity as shown by Caulfield et al. (2007) and Griessbach et al. (2010). SEM images of several different LS feedstocks are shown in Fig. 4. Powders were sputter-coated with Au-Pd and scanned with a JEOL-5610 SEM at 20 kV. There is a wide variation in particle size and shape, in addition to multiple constituents in some composite powders such as glass beads and carbon fibers. Batch-to-batch variation in powder size and shape is a known problem for DuraForm™ powders, as discussed by Gornet et al. (2002).

Example particle size distribution plots, measured by laser diffraction, are shown in Fig. 4 alongside the corresponding SEM images. Large particles tend to require more laser energy to melt than small particles, so large variations in particle size can result in complete melting of small particles and incomplete melting of large ones, as discussed by Dupin et al. (2012). This partial melting results in "cored" spherulites, and in some cases porosity.

Coring in LS is believed to be the result of the inner particle "core" being comprised of a different crystal phase than the surrounding material, and is considered by some to be major cause of LS part failure, as discussed by Zarringhalam (2009). An optical microscope image of this coring is shown in Fig. 5 (left), generated by Hopkinson et al. (2009). Coring is prevalent in LS parts, but does not show up in IM parts.

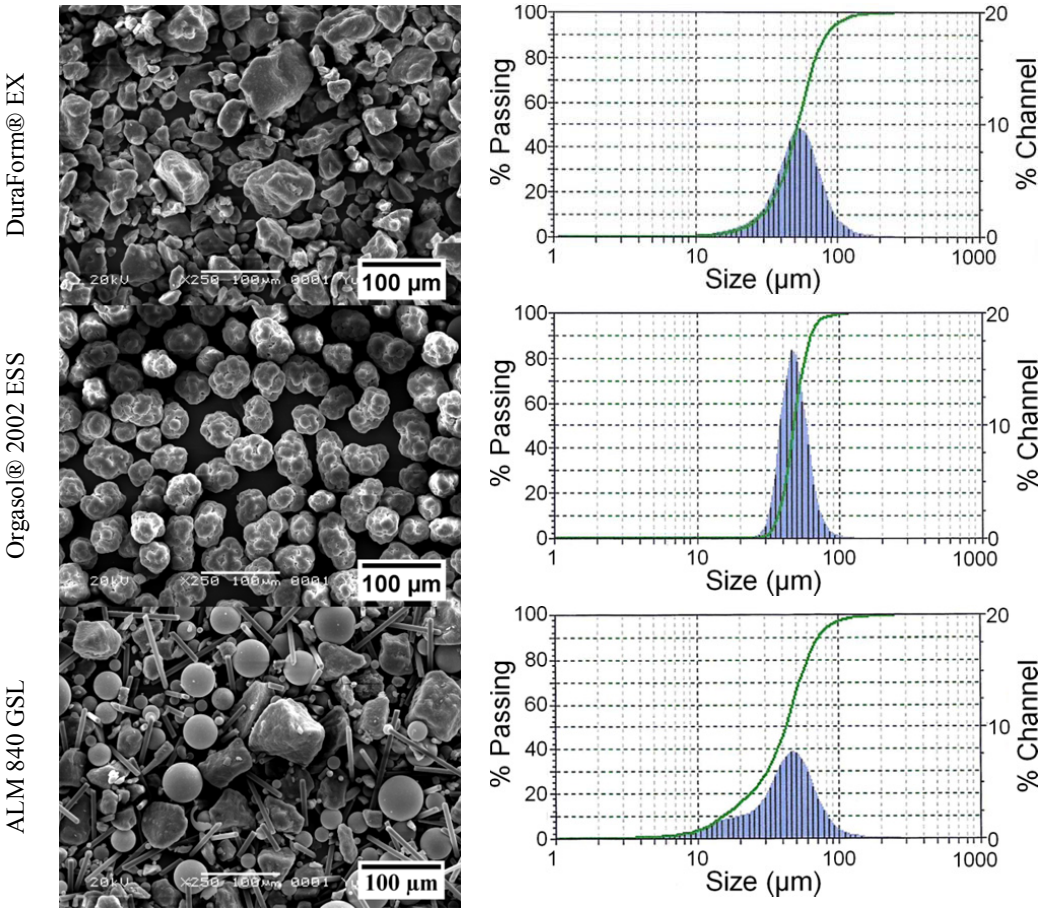

Fig. 4. SEM images and laser diffraction PSD results for three LS powders.

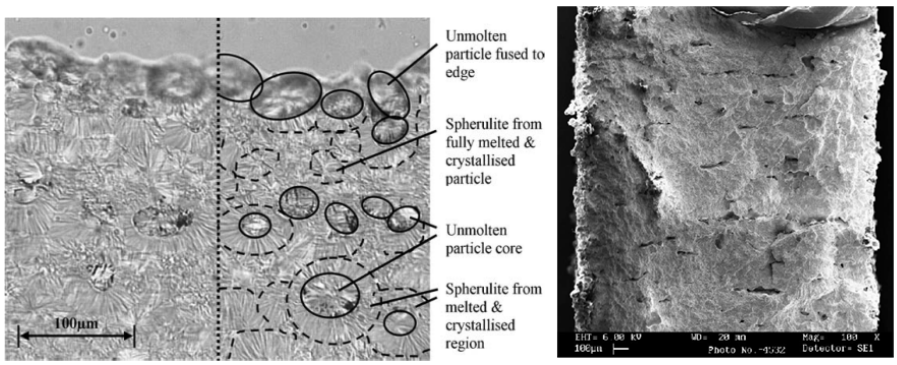

Fig. 5. (left) Optical microscope image of LS-PA12 coring, from Zarringhalam et al. (2006); (right) porous fracture surface of LS part, from Ajoku et al. (2006).

Porosity is an aspect of LS parts that is not often present in IM components. A fracture surface of an LS part with such porosity is shown in Fig. 5 (right). This porosity tends to be greater on the layer surface than inside the part, and increases with decreasing laser energy due to incomplete particle melting. Porosity can give rise to significant scatter in material properties, which is known to be a problem for LS part properties – especially elongation at break as discussed by Griessbach et al. (2010). Powder that is deposited and coalesced in layers gives rise to *normal anisotropic* mechanical properties, where the ductility normal to the powder layer is different (worse) than the in-plane directions. This is because pores tend to be aligned in the plane of the powder layers. Irregular or flaky powders result in large isolated pores and cored spherulites, while regular granular powders result in smaller aligned pores with less coring and a better surface finish; see Yusoff et al. (2011).

The strength and modulus of LS-PA parts are similar to IM-PA, but the elongation at break is typically an order of magnitude lower. For example, DuraForm™ PA has an advertised tensile strength of 43 MPa and a maximum elongation of 14%; see DuraForm (2014). This is well below the 200-300% elongation typical of IM parts. Ajoku et al. (2006) measured a higher tensile modulus and yield strength for LS parts compared to IM parts of the same PA 12 polymer. The increases in strength and modulus were presumably due to the increased degree of crystallinity (or α crystal structure) in LS parts due to the slow cooling cycle. The decreased ductility could be due to porosity and particle coring due to incomplete melting, or an increase in α-PA, degree of crystallinity, and increased spherulite size due to slow cooling. However, the greatest impact on ductility is believed to be due to prior particle boundaries, where there is little or no entanglement between neighboring spherulite crystals. This is in contrast to IM parts, where viscous shearing destroys the original particle boundaries resulting in greater entanglement.

Another concern for the behavior of LS feedstock materials is the properties of recycled powder. In laser sintering, only 10-20% of the powder in the part bed chamber is used to create the parts. The remaining powder is either swept into overflow bins, or stays in the heated part chamber to support the still-molten parts. This environment results in aging of the powder, which can limit its ability to be recycled. Mielicki et al. (2012) studied the effect of aging in N_2 on PA12 powder, and found a 10-fold increase in viscosity after approximately 20 hours at 174 °C. Other studies note a 2-3× increase in molecular weight with used powder, consistent with an increase in viscosity; see Dotchev and Yusoff (2009), and Zarringhalam et al. (2006). Since recycled powder has a higher molecular weight due to additional cross-linking, it is often mixed with virgin powder to reduce orange peel and other deleterious effects as discussed by Kruth et al. (2007). This will generally provide for adequate dimensional properties for prototype parts, but represents a problem for structural components since the aged (viscous) particles can result in incomplete melting and coalescence in the powder bed, producing porosity in the final part. The prolonged use of recycled powder ultimately results in inconsistent mechanical properties, as discussed by Choren et al. (2001).

3. Part chamber phenomena

Small variations in powder bed temperature can have a marked effect on porosity and other mechanical part properties. Variations of several degrees can be observed across typical powder bed layers using IR cameras. This is serious concern, as a 2 °C variation is a significant fraction of the 3-4 °C temperature rise needed to melt the powder. These variations are due to four causes: (1) conduction from previously heated powder layers, (2) inconsistent powder bed heating due to irregular heating elements, (3) conduction through the part cake walls, and (4) thermal convection channels that form in the N_2 atmosphere above the part bed. Fig. 6 shows two sequential part bed images in a commercial LS machine at Harvest Technologies recorded with an IR video camera. The image on the right was taken approximately 7 seconds after the image on the left. These images show temperature variations due to conduction from previous layers and through the part cake walls (left image), as well as thermal fluctuations due to convection channels (right image, lower-left corner). The convection channels form naturally due to local hot spots on the part bed surface, but are exacerbated by poor sealing of the part chamber. This is due to gradual thermal degradation of the sealing elements between the chamber door and machine frame. Poor sealing is a problem not only in terms of temperature fluctuations, but also in terms of potential oxygen exposure which could result in oxidation of the exposed part and feedstock powder. Seals are usually replaced every 4-6 weeks on commercial LS machines, based on leak rate measurements.

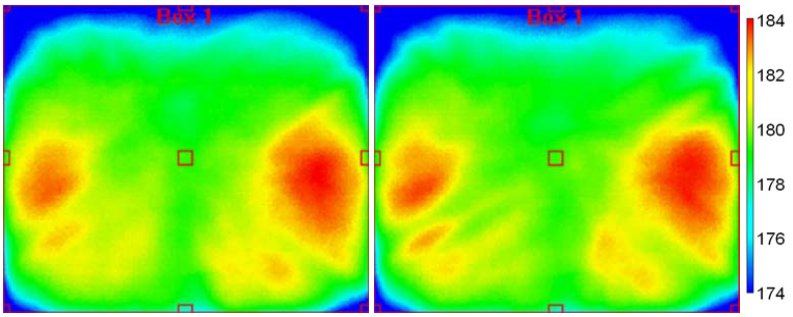

Fig. 6. Sequential IR images of top powder layer in LS machine at Harvest. The temperature range (blue-red) is 174-184 °C. Note the development of "fingers" in the lower-left quadrant of the second image due to thermal convection channels.

Another temperature concern is conduction through the part chamber walls. This is clearly evident in Fig. 6, and can result in parts with incomplete melting, porosity, and poor mechanical properties. This is particularly a problem for large builds, since the only heat sources in commercial LS machines are the laser itself, the infrared heaters above the part bed surface, and a heater below the part chamber piston. Large builds with the two regulating heat sources at either end will therefore have a larger volume in the center though which this wall cooling can serve to degrade the final part properties.

The infrared heaters used to heat and maintain the powder bed temperature have traditionally been separated into an "inner" and "outer" zone. These heating elements are typically manually-installed, can cause local hot and cold spots, and are not able to selectively heat a particular region of the part bed surface. This problem is exacerbated by the thermal convection channels and wall cooling as mentioned above. Recently, Integra (Round Rock, TX, USA) has produced a 9-zone heater layout for use in existing 3D Systems LS machines; see Integra (2014). The layout of this new heater arrangement is shown in Fig. 7 (center), and allows for an optimized thermal profile for a variety of part bed layouts. IR camera images of a part bed with a conventional 2-zone heater, and a new 9-zone heater are shown in Fig. 7 (left and right). The benefits of a tailored heating profile can include more consistent mechanical properties, less laser power required, and a lower overall part bed temperature.

Fig. 7. (left) IR camera image of part bed with two-zone heating elements; (center) photograph of multi-zone heater layout; and (right) IR camera image of part bed with multi-zone heaters. Images courtesy of Tim Gornet, Additive Manufacturing User's Group (Tucson, AZ, USA).

Another problem that arises during LS builds is "fogging" of the laser window: During the LS process, the laser beam is projected through a specially coated lens onto the part bed. This lens serves as a protective barrier to keep airborne contaminants from damaging the laser directional control mirrors. During the build, contaminants adhere to the lens, affecting the energy and shape of the laser beam. Over time the lens becomes permanently fogged, creating variability across the bed as the directional control mirrors (galvos) translate the beam around the part bed. A prototype window design was developed at Harvest to prevent this condensation through controlled heating the laser window assembly. This resulted in a decrease in output power of 3-5% over time, compared to a typical decrease of 20-25% (Fig. 8).

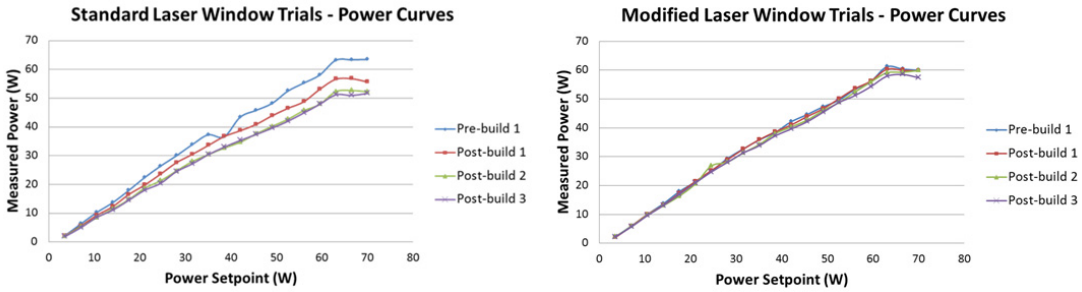

Fig. 8. Power output curves for (left) standard and (right) modified laser window collected at Harvest Technologies, Inc.

4. Commercial laser sintering machines

From a production standpoint the significant limitations to LS are part size, manufacturing speed, choice of materials, and in-situ process control. Current production LS machines are listed in Table 1. All the machines use CO_2 lasers, and are generally designed to work with low-temperature powders like polyamides. A recent exception to this is the EOSINT P 800, which has an operating temperature of 385 °C, capable of processing PEEK. EOS also produces two LS machines (EOSINT P 760, 800) that have dual sintering lasers to speed up the processing cycle. Other system improvements for 3DS and EOS include new digital scanning, better global thermal control using spot pyrometers, and improved powder supply management. Laser power monitoring is a recent feature, which is included in the EOSINT P 760/800 models to improve laser power output consistency.

The CNC interfaces to these machines are usually closed-source, so user modifications to laser control schemes are not possible. The laser sources themselves haven not changed significantly since the 1990s. Polymers only absorb laser energy in the far infrared (CO_2 lasers), and ultraviolet regimes (excimer lasers), so CO_2 laser sources are still dominant. Some research has been conducted into fiber lasers, but this is only possible if the feedstock material has special additives (e.g. carbon black) that can absorb the laser energy. To date there is no active feedback system capable of monitoring the part surface and adjusting build parameters accordingly.

Table 1. Polymer LS production machines (2014).

LS Machine	Build envelope (mm)	Layer thickness (μm)	Peak laser power	Scanning speed (m/s)	Materials
3DS sPro™ 60	381 x 330 x 437	80 - 150	30-70 W	12	PA
3DS sPro™ 140	550 x 500 x 460	80 - 150	70-200 W	15	PA
3DS sPro™ 230	550 x 550 x 750	80 - 150	70-200 W	15	PA
3DS ProX™ 500	381 x 330 x 457	80 - 150	100 W	12.7	PA
EOS FORMIGA P 110	200 x 250 x 330	60 – 120	30 W	5	PA, PS
EOS P 396	340 x 340 x 600	60 - 180	70 W	6	PA
EOSINT P 760	700 x 380 x 580	60 - 180	2 x 50 W	2 x 6	PA
EOSINT P 800	700 x 380 x 560	120	2 x 50 W	2 x 6	PA, PEEK
Farsoon 401	400 x 400 x 450	80 - 300	30 W	7.5	PA
Farsoon 402	400 x 400 x 450	80 - 300	100 W	12.7	PA
Farsoon 251	250 x 250 x 320	80 - 300	30 W	7.6	PA

5. Discussion

Most of the development efforts in production machines have gone into increasing build envelope size, processing speed, and powder management which primarily address throughput issues. Laser output monitoring is now available on some EOS machines, which periodically measures the laser power output on a reference target. Methods have been developed at Harvest Technologies to ameliorate laser window fogging, a modification that can be retrofitted to existing machines. Service companies like Integra have also developed multi-zone heaters to improve powder bed surface temperature uniformity, and advanced digital scanning retrofits for improved scanning times. All these improvements will help to improve part consistency, but there is still much that needs to be done.

The ability for rapid manufacturing of structural parts ultimately depends on the resulting microstructures. Parts must be free of porosity and particle coring if toughness values are to approach those of injection molded parts. Incomplete particle melting and coalescence is therefore a critical barrier that must be overcome. To accomplish this, advanced part monitoring and laser control schemes will likely be required. With advanced surface temperature heaters, there will still be minor (but important) temperature fluctuations in the powder layer that result in reduced or enhanced melting during scanning of the laser beam. Even if a perfectly uniform temperature exists, there will *still* be non-uniform melting and coalescence due to intrinsic powder variations such as molecular weight, particle size and shape, and crystallinity. Such hurdles require advanced powder bed monitoring and closed-loop feedback control techniques that are still to be developed.

6. Conclusions

Improvements to commercial polymer laser sintering machines in recent years have resulted in faster part generation, larger part bed chambers, improved temperature monitoring, and higher operating temperatures. In addition to this, a few service and manufacturing companies have developed solutions for processing problems such as laser window fogging and inconsistent part bed heating. However, other problems such as convection channels and part chamber wall cooling still remain. The resulting part bed temperature variations combined with irregular feedstock powder particles can result in incomplete melting, porosity, and particle coring. These microstructural defects result in inconsistent and anisotropic mechanical properties, with ductility being strongly affected. Without additional research and development into enhanced part bed monitoring and laser control schemes, these problems will likely continue and further delay the transition from rapid prototyping to rapid manufacturing

Acknowledgements

This material is based on research sponsored by the Air Force Research Laboratory, under agreement number FA8650-13-M-5061. The U.S. Government is authorized to reproduce and distribute reprints for Governmental purposes notwithstanding any copyright notation thereon. The views and conclusions contained herein are those of the authors and should not be interpreted as necessarily representing the official policies or endorsements, either expressed or implied, of the Air Force Research Laboratory or the U.S. Government.

References

Ajoku, U.; N. Hopkinson, M. Caine, “Experimental measurement and finite element modeling of the compressive properties of laser sintered Nylon-12,” *Materials Science and Engineering A*, Vol. 428, pp. 211-216, 2006.

Argon, A.S.; The Physics of Deformation and Fracture of Polymers, Cambridge University Press, New York, 2013.

Beaman, J.J.; J.W. Barlow, D.L. Bourell, R.H. Crawford, H.L. Marcus, K.P. McAlea, Solid Freeform Fabrication: A New Direction in Manufacturing, Kluwer Academic Publishers, Norwell, MA, 1997.

Bessell, T.J.; D. Hull, J.B. Shortall, “The effect of polymerization conditions and crystallinity on the mechanical properties and fracture of spherulitic nylon 6,” *Journal of Materials Science*, Vol. 10, pp. 1127-1136, 1975.

Caulfield, B.; P.E. McHugh, S. Lohfeld, “Dependence of mechanical properties of polyamide components on build parameters in the SLS process,” *Journal of Materials Processing Technology*, Vol. 182, pp. 477-488, 2007.

Choren, T.J.; V. Gervasi, T. Herman, S. Kamara, J. Mitchell, “SLS powder life study”, *Solid Freeform Fabrication Symposium*, Austin, TX, August, pp. 39-44, 2001.

Dotchev, K.; W. Yusoff, "Recycling of polyamide 12 based powders in the laser sintering process," *Rapid Prototyping Journal*, Vol. 15, No. 3, pp. 192-203, 2009.

Dupin, S.; O. Lame, C. Barres, J.-Y. Charmeau, "Microstructural origin of physical and mechanical properties of polyamide 12 processed by laser sintering," *European Polymer Journal*, Vol. 48, pp. 1611-1621, 2012.

DuraForm® PA Plastic Tech Sheet, 3D Systems.

Gibson, I.; D. Shi, "Material properties and fabrication parameters in selective laser sintering process," *Rapid Prototyping Journal*, Vol. 4, No. 4, pp. 129-136, 1997.

Goodridge, R.D.; C.J. Tuck, R.J.M. Hague, "Laser sintering of polyamides and other polymers," *Progress in Materials Science*, Vol. 57, pp. 229-267, 2012.

Gornet, T.J.; K.R. Davis, T.L. Starr, K.M. Mulloy, "Characterisation of selective laser sintering materials to determine process stability", *Solid Freeform Fabrication Symposium*, Austin, TX, August, pp. 546-53, 2002.

Griessbach, S.; R. Lach, W. Grellmann, "Structure—property correlations of laser sintered nylon 12 for dynamic dye testing of plastic parts," *Polymer Testing*, Vol. 29, pp. 1026-1030, 2010.

Hooreweder, P.V.; D. Moens, R. Boonen, J.-P. Kruth, P. Sas, "On the difference in material structure and fatigue properties of nylon specimens produced by injection molding and selective laser sintering," *Polymer Testing*, Vol. 32, pp. 972-981, 2013.

Hopkinson, N.; C.E. Majewski, H. Zarringhalam, "Quantifying the degree of particle melt in Selective Laser Sintering," *CIRP Annals – Manufacturing Technology*, Vol. 58, pp. 197-200, 2009.

Hopkinson, N.; Hague, R.; Dickens, P.; Rapid Manufacturing : An Industrial Revolution for the Digital Age. Hoboken: Wiley, 2006.

Huang, H.-X.; B. Wang, W.-W. Zhou, "Polymorphism in polyamide 6 and polyamide 6/clay nanocomposites molded via water-assisted injection molding," *Composites: Part B*, Vol. 43, pp. 972-977, 2012.

Integra Upgrades, http://www.integra-support.com/upgrades.php, Accessed April 17, 2014.

Jain, P.K.; P.M. Pandey, P.V.M. Rao, "Effect of delay time on part strength in selective laser sintering," *International Journal of Advanced Manufacturing Technology*, Vol. 43, pp. 117-126, 2009.

Kruth, J.-P.; G. Levy, F. Klocke, T.H.C. Childs, "Consolidation phenomena in laser and powder-bed based layered manufacturing," *Annals of the CIRP*, Vol. 56, No. 2, pp. 730-759, 2007.

Liu-Lan, L.; S. Yu-sheng, Z. Fan-di, H. Shu-huai, "Microstructure of Selective Laser Sintered Polyamide," *Journal of Wuhan University of Technology – Mater. Sci. Ed.*, Vol. 18, No. 3, pp. 60-63, 2003.

Majewski, C.; H. Zarringhalam, N. Hopkinson, "Effect of the degree of particle melt on mechanical properties in selective laser-sintered Nylon-12 parts," *Proceedings of the Institution of Mechanical Engineers, Part B: Journal of Engineering Manufacture*, Vol. 222, pp. 1055-1064, 2008.

Mielicki, C.; A. Wegner, B. Gronhoff, J. Wortberg, G. Witt, "Prediction of PA12 melt viscosity in Laser Sintering by a Time and Temperature dependent rheological model," *Ausgabe*, Vol. 9, 2012.

Starr, T.L.; T.J. Gornet, J.S. Usher, "The effect of process conditions on mechanical properties of laser-sintered nylon," *Rapid Prototyping Journal*, Vol. 17, No. 6, pp. 418-423, 2011.

Tontowi, A.E.; T.H.C. Childs, "Density prediction of crystalline polymer sintered parts at various powder bed temperatures," *Rapid Prototyping Journal*, Vol. 7, No. 3, pp. 180-184, 2001.

Yuan, M.; Bourell, D; Diller, T; "Thermal Conductivity Measurements of Polyamide 12," In Proceedings of the Solid Freeform Fabrication Symposium, pp. 427-437, 2011.

Yusoff, W.A.Y.; S.A. Nasir, W.M.H. Ahmad, "Investigation of the effect of "Orange Peel" surface texture on the laser sintered part," *2011 IEEE Symp. on Business, Engineering and Industrial Applications (ISBEIA)*, pp. 43-48, 2011.

Zarringhalam, H.; "Degree of particle melt in Nylon-12 selective laser-sintered parts," Rapid Prototyping Journal, Vol. 15, No. 2, pp. 126-132, 2009.

Zarringhalam, H.; N. Hopkinson, N.F. Kamperman, J.J. de Vlieger, "Effects of processing on microstructure and properties of SLS Nylon 12," *Materials Science and Engineering A*, Vol. 435-436, pp. 182-180, 2006.

Zhou, H.; Computer Modeling for Injection Molding, John Wiley & Sons, Hoboken, NJ, 2013.